Journal of Food Engineering 285 (2020) 110089

Contents lists available at ScienceDirect

Journal of Food Engineering

journal homepage: http://www.elsevier.com/locate/jfoodeng

Microencapsulation of olive leaf extract by freeze-drying: Effect of carrier composition on process efficiency and technological properties of the powders

Rodrigo González-Ortega *, Marco Faieta, Carla D. Di Mattia, Luca Valbonetti, Paola Pittia **

University of Teramo, Faculty of Bioscience and Technology for Food Agriculture and Environment, 64100 Teramo, Italy

ARTICLE INFO

Keywords:
Olive leaves
Oleuropein
Microencapsulation
Freeze-drying
Response surface
Maltodextrin

ABSTRACT

In this study the effect of matrix composition on process encapsulation efficiency, antioxidant capacity and physical properties of microencapsulated olive (*Olea europaea* L.) leaves extract (OLE) powders obtained by freeze-drying were investigated. Total solids, matrix composition (maltodextrin and trehalose, alone or mixtures) and OLE:matrix ratio of the initial aqueous system were investigated by applying a Response Surface Methodology. Results highlighted that encapsulation efficiency resulted positively affected by higher concentrations of maltodextrin and lower OLE:matrix ratio. Thermal properties were influenced by the overall composition of the powders with an increased T_g at increasing maltodextrin content while OLE had a plasticizing effect. By microscopy analysis, differences in surface and particle morphology as well as OLE distribution in the differently formulated powders were observed in agreement with the corresponding encapsulation efficiency. This study highlights the importance of formulation optimization in freeze-drying encapsulation to enhance process efficiency and the technological functionalities of the powders.

1. Introduction

Among the large variety of bioactives naturally present in foods, polyphenols, secondary metabolites of plants, have been extensively reported for their health-promoting properties as free radical scavengers (Leopoldini et al., 2011). Increasing is, thus, the interest in the development and formulation of food products made of raw materials or ingredients naturally rich in phenolic compounds as well as the implementation of processing for extraction or isolation of bioactives from diverse plant sources.

Olive leaves are an important waste stream from olive oil production, along with olive pomace and waste waters. Leaves are considered a cheap and rich source of valuable compounds that can be obtained with relatively cost-effective processes (Difonzo et al., 2017; Xynos et al., 2014). These extracts contain high amounts of bioactives like phenolic compounds, which can be classified into secoiridoids (oleuropein, verbascoside and derivatives) flavonoids (luteolin, rutin, apigenin and derivatives) and substituted phenols (hydroxytyrosol, tyrosol, caffeic and vanillic acid) (Souilem et al., 2017; Talhaoui et al., 2015) OLE and its major phenolics oleuropein and hydroxytyrosol have been consistently associated to numerous health benefits such as the prevention of oxidative-stress related (e.g. coronary heart diseases) and neurogenerative diseases, and cancer (Di Francesco et al., 2015; Martín-Peláez et al., 2013). From a techno-functional perspective, the incorporation of olive mill waste phenolic extracts into food products has been recently studied as wine antimicrobial preservative (Ruiz-Moreno et al., 2015), lipid oxidation inhibitor in meat products (Aouidi et al., 2017) or in vegetal oils for their antioxidant properties (Mohammadi et al., 2016).

Ahmad-Qasem et al. (2016) highlighted that the method for drying the olive leaves influenced the initial extract composition and bioactive potential, and extract dehydration resulted in a 10% loss of bioactivity, but the extracts remained stable for at least 4 weeks during storage at 4-35 °C. However, the use and application of such phenolic extracts often requires stabilization to avoid chemical degradation during processing and long storage and enhance solubility, but also to improve the physical stability and easiness of handling (Munin and Edwards-Lévy, 2011). Microencapsulation technologies involve those processes to pack or entrap molecules and components (core) in a matrix of a single or complex secondary material, resulting in small particles or capsules from the submicron range to several hundred microns. They are

* Corresponding author.
** Corresponding author.
E-mail addresses: rodriglez7@hotmail.com (R. González-Ortega), ppittia@unite.it (P. Pittia).

https://doi.org/10.1016/j.jfoodeng.2020.110089
Received 10 January 2020; Received in revised form 10 March 2020; Accepted 19 April 2020
Available online 21 April 2020

designed to protect and increase stability of the bioactive core material during processing, storage and consumption (Roos and Livney, 2017).

Largely used in the food sector are the microencapsulation technologies based on desolvation mechanisms like spray-drying and freeze-drying to form fine, dry powders. In particular, freeze-drying is an interesting alternative to the more commonly used spray-drying when thermosensitive molecules have to be encapsulated. Despite the advantages that spray-drying has like lower cost, higher rate and industrial flexibility, freeze-drying yields high quality products with minimal thermal and oxidative degradation and higher entrapment efficiency (Ballesteros et al., 2017; Pasrija et al., 2015). In freeze-drying, apart from process parameters, formulation factors like concentration of solutes in the initial solution, core to matrix ratio or matrix composition are known to affect the encapsulation efficiency, microstructure and the thermophysical properties (Ballesteros et al., 2017; Ravichai and Muangrat, 2019).

High and medium chain carbohydrates like starch, maltodextrins and cyclodextrins are commonly used as wall materials in encapsulation thanks to their ability to form amorphous matrices. Encapsulation of olive leaves and other waste by-products using these carriers by spray-drying (Aliakbarian et al., 2018; Paini et al., 2015; Urzúa et al., 2017) and freeze-drying (Chanioti et al., 2016; Ganje et al., 2016; Mourtzinos et al., 2007) have shown high encapsulation efficiencies, improved hygroscopicity and stability.

On the other hand, small carbohydrates like mono- and disaccharides are not so widely used for conventional encapsulation due to poorer film-forming, glass forming and thermal properties. However, trehalose (α-D-glucopyranosyl-(1 → 1)-α-D-glucopyranoside) is a natural disaccharide that is known to stabilize proteins and lipid membranes in low moisture systems and has been applied in food encapsulation of vitamins (Zhou and Roos, 2012), flavors (Sosa et al., 2011) and colorants (Faieta et al., 2019). Its bioprotective action is partly attributed to its ability to form amorphous solids and high glass transition temperature, along with other mechanism (Patist and Zoerb, 2005). Several studies have investigated the physico-chemical properties of freeze-dried amorphous mixed maltodextrin-disaccharide systems, since they are representative of many food systems like bakery products or fruit (Maidannyk et al., 2017; Potes et al., 2012). However, they have been scarcely characterized for their capacity to entrap bioactives when used in freeze-drying encapsulation and the technological properties of the resulting powders. Response surface methodology (RSM) is a robust model that can be used to determine the impact of each factor and how the factors interact, thereby the process of optimization could be efficiently performed. The RSM has been already applied in encapsulation to optimize factor interactions influencing the responses as well as the design of experiments and information obtained (Chen et al., 2019; Paulo and Santos, 2017; Ramírez et al., 2015).

The aim of this study was to study the effect of the carrier formulation on the encapsulation efficiency of an olive leaf extract rich in oleuropein, the thermal, physical and structural properties of freeze-dried microencapsulated powders. Maltodextrin and trehalose were chosen as encapsulating materials as representatives of high and low molecular weight carbohydrates with good glass forming properties for encapsulation purposes. Total solids, matrix composition (maltodextrin and trehalose, alone or mixes) and OLE:matrix ratio of the initial aqueous system were investigated by applying a Response Surface Methodology.

2. Materials and methods

2.1. Materials

A standardized olive leaf powder extract (OLE), obtained from leaves of the olive tree (*Olea europaea* L.*)* by ethanolic-aqueous maceration, was kindly provided by OLEAFIT S.r.l (Isola del Gran Sasso, Italy). Maltodextrin (MD) (DE 8–10) and trehalose dihydrate (TR) were provided by Cargill S.r.l. (Milan, Italy). Moisture of maltodextrin, trehalose and OLE determined gravimetrically (oven-drying at 105 °C for 4 h) were 8.6%, 9.2% and 4.2% (w/w) respectively and these values were taken into consideration when solutions were prepared for microencapsulation purposes. The following standard compounds were used: hydroxytyrosol (≥98% HPLC; Extrasynthese, Lyon, France), oleuropein (≥90% HPLC; PanReac AppliChem, Darmstadt, Germany) and verbascoside (≥99% HPLC; Sigma-Aldrich, Darmstadt, Germany).

All other solvents and reagents used were of analytical grade.

2.2. Experimental design for process optimization using central composite design

In order to reduce the number of trials and maximize the obtained information on the effect of encapsulating variables on product properties, a central composite inscribed design (CCI) was applied. A central composite design is a 2^k full factorial design to which the central point and the *star points (α)* are added to determine the curvature of the model. Three factors (i.e. independent variables) were selected: dispersed solids (X_1, % w/v), MD:TR matrix composition ratio (X_2, %MD) and OLE:matrix ratio (X_3) at 5 levels (Table 1); *α star points* set at a distance from the central point equal to $\alpha = \sqrt{k/k}$ were also included. The CCI consisted of 17 experiments including 3 center points, 6 *star points* and 8 factorial points.

The dependent, or response, variables were the following: Total Phenolic Content (TPC) encapsulation efficiency (Y_1, TPC-EE%) and oleuropein encapsulation efficiency (Y_2, Oleu-EE%). Preparation of formulations and analysis were randomized to avoid experimental biases. Design Expert® Software (V.7.0, Stat-Ease Inc., Minneapolis, USA) was used for the generation and evaluation of the statistical experimental design and generate the response surface plots. Experimental data obtained were fitted to the following second order polynomial equation (**Eq. (1)**):

$$Y_{1-2} = a_0 + a_1X_1 + a_2X_2 + a_2X_2 + a_3X_3 + a_{12}X_1X_2 + a_{13}X_1X_3 + a_{23}X_2X_3 + a_{11}X_1^2 + a_{22}X_2^2 + a_{33}X_3^2 \quad (1)$$

where Y ($_{1-2}$) are predicted response values for each of the dependent variables; a_0 is the regression coefficient at the center point; a_1, a_2 and a_3

Table 1
Independent variables and levels of the central composite design.

Coded values	Independent variables		
	X_1	X_2	X_3
	% solids (w/v)	MD:TR[a] (%MD)	OLE:matrix[b]
Low (−1)	10	0	0.05
Medium (0)	20	50	0.15
High (+1)	30	100	0.25
-∝ (−0.57)	14	21	0.09
+∝ (+0.57)	26	79	0.21

[a] Matrix composition expressed as % MD (%TR = 100-%MD).
[b] OLE to matrix ratio (MD + TR) MD: maltodextrin, TR: trehalose.

are linear coefficients; a_{12}, a_{13} and a_{23} are second order factors; and a_{11}, a_{22}, a_{33} are quadratic coefficients. X_1, X_2 and X_3 are the independent variables.

2.3. Preparation of freeze-dried microencapsulated olive leaf extract powders

Matrix components (MD and/or TR) were initially dissolved in ultrapure water at 20 °C and stirred at 200 rpm for 60 min until clear transparent solutions were obtained. Then, OLE was slowly added and the mix was stirred at 350 rpm for 30 min. The obtained dispersion was centrifuged at 4000 rpm for 30 min and subsequently filtered through 0.45 μm Nylon filter (47 mm, Whatman®, GE Healthcare) to remove insoluble material and obtain clear solutions. Each solution was transferred into Petri dishes and frozen at −80 °C for at least 14 h and freeze-dried (CoolSafe Scanvac, LaboGene, Allerod, Denmark) for 74 h at a pressure < 0.4 mbar using a temperature ramp starting from −42 °C up to 20 °C optimized according to the T_g and T'_g of the initial aqueous systems. Dried samples were then ground using a planetary ball mill (Pulverisette 6, Fritsch, Weimar, Germany) with a zirconium oxide grinding bowl (80 mL) and grinding balls (10 mm diameter) at a disk speed of 350 rpm for 30 s under low relative moisture conditions. Powdered samples were stored in vacuum desiccators over P_2O_5 (VWR Chemicals, Milan, Italy) until constant weight before further use. Freeze-dried matrices without OLE were also prepared using the same procedure, and used as control samples. These samples were subjected to all the analyses except the confocal microscopy analysis. For confocal laser scanning microscopy analysis, microencapsulated powders at 30% (w/v) of dispersed solids, three different OLE addition (ratio OLE:matrix = 0.05, 0.15 and 0.25) and three different carrier composition formulations (maltodextrin, trehalose and maltodextrin-trehalose mix at 1:1 wt ratio) were also prepared as above described, in order to compare samples based on the matrix composition and three levels of OLE concentration.

2.4. Estimated encapsulation efficiency (EE) and load yield (Y)

Encapsulation efficiency is defined as the TPC and oleuropein (as %) that is entrapped in the matrix of wall material after freeze-drying in respect to that present in the initial system. It has been determined by adapting the method and equations presented by other authors (Laine et al., 2008) on the microencapsulated products by exactly weighing an amount of each powder (ca. 15–20 mg) on microcentrifuge tubes to which 1.4 mL absolute ethanol was added. Powder suspension was immediately vortexed (10 s) and centrifuged at 12000*g* for 2 min (Eppendorf Centrifuge 5415D). The supernatant ethanol fraction was collected and the pellet was dissolved in 1.4 mL of water by vortexing. Both fractions were analyzed for TPC, oleuropein content, and TEAC antioxidant capacity was measured on the encapsulated fraction.

Phenolic compounds in the ethanol fraction were considered to be surface/non-encapsulated fraction, while phenolics in the water fraction correspond to the encapsulated fraction.

The encapsulation efficiency (EE) for total phenolics content and oleuropein was calculated according to **Eq. (2)**:

$$\text{EE}\ (\%) = \frac{\text{Encapsulated phenolics (mg/g powder)}}{\text{Encapsulated phenolics (mg/g powder)} + \text{Surface phenolics(mg/g powder)}} \text{x}100 \quad (2)$$

The load Yield (Y), indicating the amount of phenolic compounds (TPC or Oleuropein) initially added still present in the microencapsulated matrix after the freeze-drying process, was computed according to **Eq. (3)**:

$$\text{Y}\ (\%) = \frac{\text{Total phenolics (encapsulated + surface)(mg/g powder)}}{\text{Calculated value of added phenolic (mg/g powder)}} \text{x}100 \quad (3)$$

2.5. HPLC determination of phenolic compounds

The content of the main phenolic compounds (oleuropein, verbascoside and hydroxytyrosol) in OLE and oleuropein in microencapsulated OLE powders were determined by adapting the method of Ahmad-Qasem et al. (2013), by high performance liquid chromatography (HPLC 1200 Infinity, Agilent Technologies, CA, USA) equipped with a C18 column (250 × 4.6 mm; 5 μm, Kinetex, Phenomenex, CA, USA) connected with a UV-diode array detector. Elution was carried out at 30 °C column temperature, flow rate 0.8 mL/min and 20 μL injection volume. The mobile phases consisted of (A) 2.5% acetic acid and (B) acetonitrile and separation was performed with the following gradient: 0–10 min, 10–20% B; 10–35 min, 20–40% B; 35–40 min, 40–100% B; 40–45 min, 100% B; 45–46 min, 100-10% B; 46–52 min, 10% B. Detection was done at 280 nm for hydroxytyrosol and oleuropein, and 330 nm for verbascoside and the corresponding concentration determined by calibration curves of the pure standard compounds.

2.6. Total phenolic content (TPC)

The TPC of OLE and microencapsulated OLE powders was evaluated by using the Folin-Ciocalteu reagent, in agreement with the method modified by (Sacchetti et al., 2009). Solutions with resuspended microencapsulated powders (0.1–0.4 mL) were diluted with deionized water to a volume of 5 mL, added with 0.5 mL Folin-Ciocalteu reagent (Sigma-Aldrich, Darmstadt, Germany) and then incubated for 3 min in the dark before adding 1.5 mL of a 25% (w/v) Na_2CO_3 solution. Then, deionized water was added to a final volume of 10 mL. The reaction mix was kept in the dark at room temperature for 60 min and total phenolic content was determined by reading the absorbance at 765 nm using a spectrophotometer (PerkinElmer Lambda Bio 25, Boston, MA, USA). Gallic acid standard (Sigma-Aldrich) solutions were used to calibrate the analysis, and results were expressed as mg of gallic acid equivalents g^{-1} of dry weight of sample. Each sample was analyzed in triplicate.

2.7. Antioxidant capacity (TEAC)

The antioxidant capacity was determined on the OLE encapsulated powders, according to the radical scavenging method described by (Re et al., 1999), with slight modifications. The $ABTS^+$ radical was generated by reacting a 7 mM solution of ABTS (2,2′-Azino-bis(3-ethylbenzothiazoline-6-sulfonic acid) diammonium salt, ≥98% HPLC, Sigma-Aldrich) with 2.45 mM potassium persulfate and allowing the mixture to stand in the dark at room temperature for 14–16 h before use.

This $ABTS^{+}$ stock solution was diluted with water to have an absorbance of 0.70 ±0.02 at 734 nm at 30°C. Three different dilutions of each sample were prepared and 30 μL added to 2.97 mL of appropriately diluted $ABTS^{+}$ solution; the absorbance decrease at 734 nm was then read after 7min. For each dilution, the percentage of inhibition was calculated as $((Abs_{initial} - Abs_{final})/Abs_{initial} \times 100)$. The % inhibition was plotted as a function of concentration and the Trolox Equivalent Antioxidant Capacity (TEAC) was calculated as the ratio of the linear regression coefficient of the sample and that of Trolox standard (6-Hydroxy-2,5,7,8-tetramethylchromane-2-carboxylic acid, ≥97%, Sigma-Aldrich). Results were expressed as μmol Trolox equivalents g^{-1} (μmol TE g^{-1}).

2.8. Thermal analysis

Thermal analysis of the powders was carried out by using a differential scanning calorimeter (DSC 8500, PerkinElmer, Waltham, MA, USA) adapting the method reported elsewhere (Maidannyk et al., 2017). Analysis were carried out to determine the glass transition temperature (T_g) of amorphous freeze-dried powders with and without encapsulated OLE. An aliquot of the powder accurately weighed (ca. 5–7 mg) was placed into DSC aluminium pans (50 μL, PerkinElmer) and hermetically sealed with pierced aluminium lids to allow evaporation of residual water upon heating scan measurement. Samples were scanned from ~30°C below to approximately 50°C above the glass transition temperature (T_g) at 5°C/min heating rate and cooled at 10°C/min cooling rate to initial temperature. A second heating scan at 5°C/min was used to determine the onset and change of specific heat at T_g (ΔCp) using the Pyris™ software (PerkinElmer).

2.9. Color of microencapsulated powders

Color of the freeze-dried powders were determined by using a benchtop spectrophotocolourimeter (Chroma Meter CR-5, Konica Minolta, Osaka, Japan) with pulsed xenon light as light source and standard illuminant D65. An aperture size of 3 mm was used. Colorimetric results are expressed in CIE L*a*b* color space, as L*(lightness), a*(red *vs* green), and b*(yellow *vs* blue) values; and the Yellow Index (YI) was calculated as follows, YI = 142.86 b*/L* (Francis and Clydesdale, 1975).

2.10. Confocal laser scanning microscopy analysis

OLE distribution in the freeze-dried powders was evaluated by using a Nikon A1-R confocal imaging system (Nikon Corp., Tokyo, Japan) controlled by Nikon NIS Elements interface, equipped with a Plan Apo λ 10X/40X Oil objective (numerical aperture: 0.3/1.5; refractive index: 1.55). In order to visualize the natural fluorescence phenolic compounds, as reported in similar studies (Pravinata and Murray, 2019), samples were excited at 488 nm and fluorescence was detected in the green channel signal at λ_{em}=500/550 nm, and observed with Nikon A1 Piezo Z Drive, pinhole size of 25.5 μm and Z-step of 1 μm.

2.11. Scanning electron microscopy (SEM) analysis

The freeze-dried powders microstructure and surface morphology were assessed by using a field-emission scanning electron microscope (SEM) LEO 1525 (ZEISS, Germany). Prior to image acquisition, sample powders were mounted on stubs and coated with a thin layer of chromium. Acceleration potential voltage was maintained between 10 keV and 15 keV.

2.12. Statistical analysis

Results are expressed as mean±standard deviation (SD) of at least three replicates for each of the 17 experimental samples of the CCI. One-way ANOVA was applied to estimate the significance of the model ($p<0.05$), effects of variables and lack of fit (Design Expert® Software V.7.0, Stat-Ease Inc., Minneapolis, USA). Data of the T_g of powders, with and without encapsulated OLE, were compared with paired *t*-test ($p<0.05$), while color analysis by an ANOVA Tukey's multiple comparison test ($p<0.05$) using R v3.5.3 and RStudio v1.1.463 (RStudio, Inc., Boston, MA, USA).

3. Results and discussion

3.1. Phenolic characterization of OLE

The olive leaf extract used in this study had a total phenolic content of 403 ±23 mg GAE g^{-1} of powder. Oleuropein, representing 80.8 ± 0.6% of the total chromatographic peak area at 280nm resulted the main phenolic compound with a concentration equal to 525 ±27 mg g^{-1}

Table 2
Experimental plan of inscribed central composite design (coded variables in brackets) with observed response variables $Y_{1\text{-}2}$, and total phenolic yield, oleuropein yield and Trolox antioxidant capacity (TEAC) values.

EF	Levels of independent variables			EE (%)		Yield (%)		TEAC (Enc)[a] (μmol TE g^{-1})
	(X_1)	(X_2)	(X_3)	TPC (Y_1)	Oleu (Y_2)	TPC	Oleu	
1	10	0	0.05	57.73 ±1.13	55.35 ±1.25	73.48 ±1.30^{bd}	85.26 ±1.29^{dfg}	43.67 ±4.08^{a}
2	30	0	0.05	64.83 ±0.33	55.10 ±1.56	75.22 ±0.99^{d}	92.01 ±2.77^{fh}	45.69 ±2.06^{ab}
3	10	100	0.05	98.51 ±0.14	99.23 ±0.16	70.73 ±1.74^{abc}	73.29 ±3.46^{ab}	65.41 ±1.85^{bc}
4	30	100	0.05	99.33 ±0.18	99.88 ±0.10	70.21 ±0.60^{ab}	72.15 ±1.73^{a}	69.78 ±6.45^{c}
5	10	0	0.25	38.61 ±1.52	29.32 ±1.03	73.11 ±1.22^{ad}	95.78 ±3.53^{h}	113.70 ±9.27^{de}
6	30	0	0.25	50.22 ±1.05	39.61 ±1.36	72.58 ±0.52^{ad}	85.89 ±0.51^{dfg}	136.87 ±6.81^{f}
7	10	100	0.25	81.07 ±0.75	74.80 ±0.67	71.97 ±1.39^{ad}	84.54 ±2.79^{df}	214.04 ±13.56^{g}
8	30	100	0.25	86.61 ±0.56	82.12 ±0.91	70.78 ±1.05^{abc}	79.46 ±3.68^{ade}	220.48 ±6.61^{g}
9	14	50	0.15	74.96 ±0.26	65.76 ±2.11	72.09 ±2.14^{ad}	77.84 ±3.80^{ad}	132.26 ±9.16^{ef}
10	26	50	0.15	78.85 ±0.58	70.59 ±0.32	73.72 ±1.66^{bd}	81.38 ±2.05^{bde}	132.57 ±5.49^{ef}
11	20	21	0.15	54.09 ±0.58	43.38 ±1.64	74.34 ±0.66^{cd}	93.50 ±0.86^{gh}	100.06 ±3.04^{d}
12	20	79	0.15	91.60 ±0.30	87.78 ±0.68	69.11 ±0.92^{a}	75.41 ±4.11^{abc}	150.09 ±1.12^{f}
13	20	50	0.09	85.90 ±1.11	77.12 ±1.86	72.61 ±2.50^{ad}	83.39 ±1.61^{cde}	98.67 ±1.85^{d}
14	20	50	0.21	68.06 ±0.68	58.82 ±0.82	71.92 ±1.75^{ad}	84.04 ±1.55^{df}	149.59 ±12.57^{f}
15	20	50	0.15	75.20 ±0.26	68.69 ±1.12	72.32 ±0.31^{ad}	86.88 ±3.85^{efg}	134.25 ±5.17^{f}
16	20	50	0.15	77.64 ±0.84	71.72 ±0.40	72.81 ±0.67^{ad}	84.21 ±0.78^{df}	137.56 ±4.85^{f}
17	20	50	0.15	76.94 ±1.03	69.42 ±1.50	73.48 ±1.30^{bd}	83.77 ±3.24^{df}	136.35 ±2.61^{f}

EF: Experimental formulation; EE: Encapsulation efficiency; TPC: total phenolic content; Oleu: oleuropein; MD: Maltodextrin; TR: trehalose.
Results are expressed as mean value of three replicate analysis ±SD. Different superscript letters in the same column indicate significant differences at a probability level of $p < 0.05$.
[a] TEAC of encapsulated fraction of microencapsulated powders.

Table 3
Analysis of variance (ANOVA) of independent variables for the optimization of response variables.

Source	Sum of squares	Degree of freedom	Coefficient	Mean square	F-value	*P*-value
Y_1: TPC-EE (%)						
Model	4361.99	4		1090.50	70.10	<0.0001
X_1- Solids (% w/v)	86.09	1		86.09	5.53	0.0365
X_2- MD:TR (% MD)	3565.28	1		3565.28	229.20	<0.0001
X_3- OLE:matrix	635.05	1		635.05	40.83	<0.0001
X_2^2	75.57	1		75.57	4.86	0.0478
Residual	186.66	12		15.56		
Lack of fit	183.51	10		18.35	11.63	0.0818
Pure error	3.16	2		1.58		
Cor.Total R^2	4548.66	16				
R^2			0.959			
Y_2: Oleu-EE (%)						
Model	5753.46	2		2876.73	130.51	<0.0001
X_2- MD:TR (% MD)	4725.80	1		4725.80	214.40	<0.0001
X_3- OLE:matrix	1027.66	1		1027.66	46.62	<0.0001
Residual	308.59	14		22.04		
Lack of fit	303.59	12		25.30	10.12	0.0934
Pure error	5.00	2		2.50		
Cor.Total R^2	6062.05	16				
R^2			0.949			

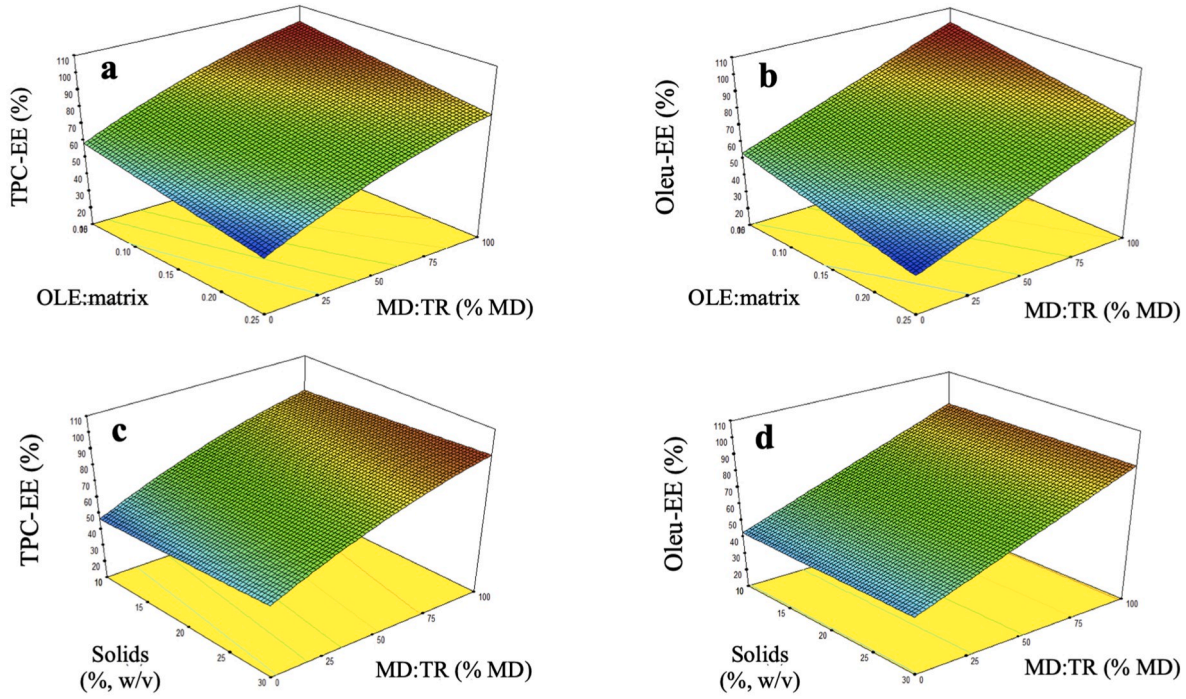

Fig. 1. 3D iso-response contour plots for encapsulation efficiency of total phenolic content (TPC-EE, %) (a, c) and oleuropein (Oleu-EE, %) (b, d) as affected by independent variables OLE:matrix ratio and MD:TR ratio (a-b) or total dispersed solids and MD:TR ratio (c–d).

extract, while verbascoside and hydroxytyrosol were found to have a concentration of 14.3 ±1.0 mg g^{-1} and 3.8 ±0.3 mg g^{-1} extract, respectively. The antioxidant capacity was found equal to 950 ±51 μmol TE g^{-1} as determined by the $ABTS^+$ assay.

3.2. Experimental design and fitting of model

The implemented CCI generated 17 experimental formulations (EF). Table 2 shows an overview of the different formulations with the factor levels and the observed values for the response variables ($Y_{1\text{-}2}$). Two quadratic polynomial equations with main and interaction factors were obtained and reduced models were applied by removing not significant factors. Both models were found to be significant ($p<0.05$) and the coefficient of determination (R^2) (Table 3), adjusted R^2, predicted R^2 and predicted residual sum of squares (PRESS) were also satisfactory (*data not shown*). The analysis of error indicated that lack of fit was not significant ($p>0.05$) for model responses, assuming the validity of the model (Myers et al., 2016) to predict and optimize variables for encapsulation of OLE phenolic compounds in carbohydrate glassy matrices.

3.3. Variable effects on encapsulation efficiency of OLE (TPC and Oleu)

The effect of process factors (% solids, MD:TR ratio and OLE:matrix ratio) on encapsulation efficiency of total phenolic compounds (TPC-EE, %) are shown in the 3D response contour plots (Fig. 1a and **1c)** resulting from the application of the RSM regression equation (**Eq. (4)**):

$$Y_1 - (TPC - EE\%) = 76.40 + 3.15X_1 + 20.28X_2 - 8.56X_3 - 4.56X_2^2 \quad (4)$$

The results of ANOVA (Table 3) indicate that the TPC-EE% was affected by all three factors ($p<0.05$), although the impact of the total dispersed solids (X_1) ($p<0.0365$) was less significant than the other two (X_2, MD:TR; X_3, OLE:matrix), with a slight increase in TPC-EE with higher total solids.

In general, carbohydrate solutions with higher solute concentration result in freeze-dried powders with lower porosity and higher bulk density after sublimation of water crystals during freeze-drying with consequent lower surface to mass ratio of dry material and subsequent reduced exposure of the surface bioactive fractions (Desobry et al., 1997; Michalska and Lech, 2018). Several studies on freeze-drying (Saikia et al., 2015) and spray-drying (Igual et al., 2014) microencapsulation of fruit extracts have shown that higher total solute concentration along with a higher ratio of encapsulant-to-core material ratio resulted in improved entrapment of bioactive compounds. On the other hand, other authors in a study on encapsulation by freeze-drying using gum arabic and maltodextrin as encapsulants, found higher recovery of total phenolics at 10–20% encapsulant concentration compared to 30% (Ramírez et al., 2015). However, this effect was not seen in samples in which maltodextrin was the dominant or only wall component, where increasing concentration resulted in higher retention. This may indicate that nature of the wall material components can have a deep impact on the retention of phenolic compounds as they can significantly affect the structuring of the matrix and the wall-core interactions.

Matrix composition and its quadratic term resulted to have a higher impact, with a higher TPC-EE% at increasing maltodextrin content. In general, a higher maltodextrin fraction in microencapsulated powders carrier composition resulted in a higher EE% for phenolic compounds. For example, 100% maltodextrin carrier system (EF 8), showed an EE % equal to 86, significantly higher than its equivalent EF 6, made out of 100% trehalose carrier (EE 50%). Other studies in which phenolic extracts were encapsulated in maltodextrin matrix at various dextrose equivalent values, demonstrated that better yields and encapsulation performances are obtained when higher molecular weight carbohydrates are used (Che Man et al., 1999; Laine et al., 2008; Laokuldilok and Kanha, 2017). This may indicate that phenolic compounds may be involved in stronger interactions with large carbohydrate polymers, and this may also be affected by the charge, solubility and molecular mobility of the phenolic compounds considered. On the other hand, it has been suggested that the presence of small sugars in amorphous polysaccharides could induce a reduction in the number of molecular entanglements in the matrix, without significantly changing its structure or packing of the glass (Kilburn et al., 2005), with consequent decrease of the encapsulation efficiency.

The ratio of bioactive core-to-matrix carrier (OLE:matrix, X_3) was also a significant factor. The lower the ratio (i.e., the higher the matrix weight fraction in respect to the bioactive core material), the higher the encapsulation efficiency. However, the encapsulation efficiency remained high (75–82%) even at the highest (0.25) OLE:matrix ratio for samples containing maltodextrin as a sole matrix component.

The positive effect on encapsulation efficiency with increasing fraction of wall material in respect to encapsulated core has been observed in several previous studies addressing microencapsulation in carbohydrate glassy matrices of phenolic compounds also including OLE by spray-drying (González et al., 2019; Urzúa et al., 2017). As expected, a higher carbohydrate matrix fraction provides a higher number of available binding sites to interact, generally by hydrogen bonding, with phenolic compounds like oleuropein (Amoako and Awika, 2016; Gharsallaoui et al., 2007).

As regards oleuropein encapsulation, EE % values were slightly lower compared to those of TPC. However, data (Fig. 1b and **d)** resulted significantly modelled by the following RSM regression equation (**Eq. (5)**):

$$Y_2 - (Oleu - EE\%) = 67.58 + 23.35X_2 - 10.89X_3 \quad (5)$$

The factors affecting significantly the response were found to be similar as for TPC-EE. OLE:matrix ratio and wall composition (MD:TR ratio) linear effects were found as the only significant factors, being the latter the more significant (F=214.40). Again, increasing the percentage of maltodextrin in respect to trehalose as wall component and the lower core-to-encapsulant ratio resulted in enhanced entrapment.

Encapsulation values of TPC and oleuropein were in agreement with similar studies using freeze-drying (Chanioti et al., 2016) and spray-drying to encapsulate olive leaf extract (González et al., 2019; Urzúa et al., 2017) and olive pomace extracts (Aliakbarian et al., 2018). It is then confirmed that process variables with greater impact on encapsulation of polyphenols are wall material composition and core to wall ratio as reported in previous similar studies (Robert et al., 2010; Saikia et al., 2015).

3.4. Load yield and antioxidant capacity of encapsulated OLE fraction

Freeze-dried encapsulated powders had a total phenolic content (encapsulated + surface) ranging from 13.6 ±0.1 to 56.7 ±0.9 mg GAE g^{-1}, and a total oleuropein content from 18.2 ±0.4 to 96.8 ±3.6 mg oleuropein g^{-1} (*data not shown*). Load yield gives an estimation of the percentage of the initial TPC and oleuropein recovered in the powders after freeze-drying. TPC-Yield values obtained for the 17 experimental formulations were around 70% (Table 2), indicating a relatively high yield without remarkable differences among the different formulations. Similar yield values have been previously reported in freeze-dried encapsulated extracts from vegetables (Che Man et al., 1999; Laine et al., 2008). Losses may be attributed to precipitation of compounds poorly soluble in water that are present in the OLE and measured as TPC by the Folin-Ciocalteu assay, but that are removed during solubilization, centrifugation and filtration of sample solutions.

Oleuropein yield values were notably higher than TPC in the range of 72–95%, since oleuropein is highly water soluble and a smaller fraction is lost during processing. Yield was significantly higher in samples containing only trehalose compared to those with maltodextrin,

Table 4
Thermal properties (glass transition, T_g onset; and change of specific heat, ΔCp) of OLE microencapsulated and control powders.

EF	Experimental values of variables				Control samples		OLE microencapsulates	
	(X_1) % solids	(X_2) MD:TR % MD	% TR	(X_3) OLE: matrix	T_g onset (°C)	ΔCp (J g^{-1} °C $^{-1}$)	T_g onset (°C)	Δ Cp (J g^{-1} °C $^{-1}$)
2	30	0	100	0.05	98.5 ±0.2	0.48 ±0.01	102.9 ±2.1*	0.48 ±0.02
6	30	0	100	0.25			97.6 ±0.8	0.51 ±0.02
1	10	0	100	0.05	98.4 ±1.5	0.51 ±0.02	101.6 ±2.4*	0.53 ±0.05
5	10	0	100	0.25			97.0 ±1.6**	0.47 ±0.03
13	20	50	50	0.09	131.2 ±0.2	0.42 ±0.03	127.3 ±1.4*	0.34 ±0.02
15	20	50	50	0.15			122.3 ±1.3**	0.32 ±0.01
14	20	50	50	0.21			121.9 ±0.7**	0.32 ±0.01
11	20	21	79	0.15	111.5 ±0.2	0.41 ±0.10	107.0 ±0.5*	0.44 ±0.02
12	20	79	21	0.15	174.5 ±1.9	0.27 ±0.12	154.7 ±1.8**	0.19 ±0.05

$p < 0.05$ (*); $p < 0.01$ (**);$p < 0.001$(***).
Results are expressed as mean values of three replicate analysis ±SD and asterisques following T_g onset values indicate significant differences with their corresponding control sample after paired *t*-test at $p < 0.05$.

probably as a consequence of a lowering effect on water polarity. It has been observed that sugars and other small molecules (e.g. glycerol) alter water structure and its dielectric constant (Sajadi et al., 2010; Te et al., 2010), imparting a reduced solvent polarity. These phenomena have been exploited to extract phenolic compounds from food matrices with positive results (Mouratoglou et al., 2016; Paradiso et al., 2016).

The antioxidant radical scavenging capacity of encapsulated fraction of powders was in agreement with the initial OLE added and the encapsulation efficiency, showing a close correlation (R^2=0.994) with the phenolic content entrapped in the glassy matrices. As expected, powders with highest encapsulation efficiency were also those with the lowest OLE:matrix ratio, meaning a lower phenolic content (and corresponding lower antioxidant capacity) per mass unit. Thus, in practical applications a compromise between high encapsulation (higher stability) and bioactive load must be reached.

3.5. Thermal properties

The knowledge of the glass transition temperature of a system and its variation as a consequence of either matrix modification or enrichment with bioactive components represents one of the most important landmark for predicting the physical and chemical stability of low-moisture foods (Roos and Drusch, 2015; Roos and Karel, 1990).

Anhydrous T_g values of microencapsulated OLE powders and their corresponding control matrices (without OLE) are summarized in Table 4. It must be pointed out that no step change indicative of glass transition was found in the thermograms of the powders made of maltodextrin as wall component, but from literature values it can be assumed to be around 175-180°C (Roos and Karel, 1991a). The lack of a clear state transition has been previously reported for maltodextrins and attributed to the large molecular weight, heterogeneity, and very low molecular mobility in anhydrous conditions (Nurhadi et al., 2016; Roos and Karel, 1991a). In two-component maltodextrin-trehalose powders a single transition was observed confirming the miscibility of the two matrix carbohydrates (Kalichevsky and Blanshard, 1992; Maidannyk et al., 2017).

Glass transition of maltodextrin-trehalose mixtures was higher than that found in the samples made of trehalose as single component (~100°C) and increased with increasing weight fraction of maltodextrin, ranging from 111°C to 175°C. It is well defined that T_g of anhydrous homopolymers is determined by their molecular weight (Avaltroni et al., 2004; Roos and Karel, 1991b), and glasses of miscible polysaccharides-sugar have glass transitions in between the T_g of single components (Roos and Karel, 1991a).

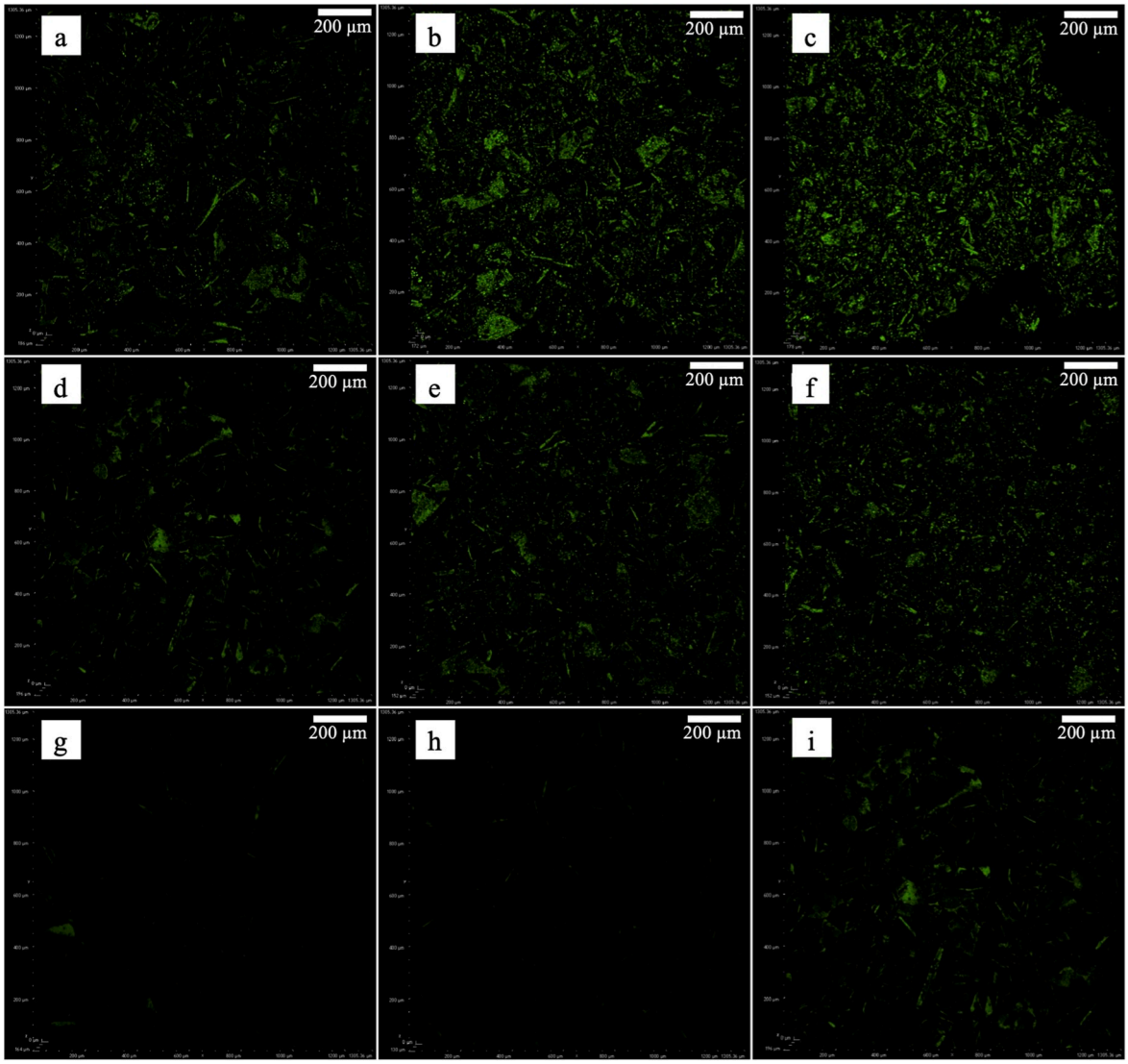

Fig. 2. CLSM micrographs of selected microencapsulated powders at (g–i) OLE:matrix ratio 0.05, (d–f) 0.15 ratio and (a–c) 0.25 ratio. Left column micrographs (a, d, g) show samples with 100%MD matrix, (b, e, h) samples with 50%MD-50%TR and (c, f, i) with 100%TR. Micrographs were taken at 10x magnification in 3D Z mode.

The effect of a third component (i.e. OLE) on the T_g resulted in a decrease of the glass-to-rubber transition temperature as a result of the plasticizing effect of the low molecular weight phenolics present in the core material. Indeed, as it can be observed in samples with increasing OLE:matrix ratio (50MD:50TR samples) a higher lowering effect of OLE on T_g was noticed. Similar plasticizing effect has been observed in maltodextrin-encapsulated cloudberry extract (Laine et al., 2008), inulin-encapsulated orange juice (Saavedra-Leos et al., 2014) and chitosan-encapsulated OLE spray-dried (Kosaraju, D'ath, & Lawrence, 2006). Surprisingly, no remarkable plasticizing effect of OLE was observed in samples with trehalose as a sole component of matrix compared to their analogous reference samples. Zhou and Roos (2012) encapsulated water-soluble vitamins in trehalose amorphous matrices and in samples at a_w=0 observed a significant decrease in T_g of around 5 to 8°C. It has been suggested that low molecular weight sugars and similar compounds acts as plasticizers of amorphous polysaccharides without changing packing or density, but by reducing molecular entanglements (Kilburn et al., 2005). Based on the molecular size of the components of OLE, the effect of this extract on the T_g of OLE-encapsulated in maltodextrin-rich systems could be similar so to allow the formation of more complex entanglements between the large carbohydrate molecules upon glass formation.

3.6. Microdistribution of OLE in encapsulated powders

Natural fluorescence of phenolic compounds present in OLE (Sikorska et al., 2012) allowed the evaluation of the phenolic fraction distribution in the carrier matrix of maltodextrin-trehalose powders, either as single or mixed binary systems. Fluorescence of the OLE and pure oleuropein were also tested under the same conditions (*images not shown*), confirming an intense green emission.

In Fig. 2 the images of the microencapsulated powders show that at increasing concentration of OLE in (OLE:matrix ratio 0.05, a-c; ratio 0.15, d-f; ratio 0.25, g-i) a stronger green signal could be noticed. Moreover, an increased trehalose content in the matrix resulted in higher signal (Fig. 2 and 100% MD, 1st column; 50-50% mixture, 2nd column; 100%TR, 3rd column). This may be due to presence on the surface of the powder bricks of a higher fraction of phenolics not entrapped in the dense amorphous carrier in agreement with the corresponding EE%. With increasing MD fraction, the higher OLE encapsulation depresses or quenches the fluorescence emission as compared to surface fraction.

In all samples in the images at a smaller scale (Fig. 3), round spots of a few micrometers with higher signal were observed. Even though signal appeared to be distributed in the whole matrix, this may be due to a fraction of OLE phase separated at a microscale level, without any evidence of structural collapse/stickiness at a macroscale level.

3.7. Morphology

Structural properties of the freeze-dried matrices are primarily formed during freezing and affect porosity and strength of solids of freeze-dried foods as well as entrapment of functional food components (Roos, 2010). In all experimental formulations after freeze-drying, a porous cake was obtained due to the sublimation of the ice, giving rise to a structure made of a glassy matrix containing air cells whose size and shape depend on the processing conditions used and composition of the initial system.

By grinding, freeze-dried systems originate powders with particles of irregular size and shape, preserving partly the initial cell-like structure and walls characteristics. In Fig. 4, SEM micrographs of freeze-dried powders made of 100% MD (Fig. 4a) or TR (Fig. 4d) alone (control), or at increasing encapsulated OLE, are shown. TR particles showed less clear pores, slightly thicker and denser cell walls and smoother surface than the MD ones that, on the contrary, present a sharper and a more structured porous morphology (Harnkarnsujarit et al., 2012). In general powders with encapsulated OLE are characterized by a rougher surface with budlike spherical domains (Fig. 4c,f) similar to those observed in CLSM micrographs.

It could be hypothesized that a fraction of the OLE dispersed in the carrier solution separated at a microscale level during the drying process, without any evidence of structural collapse/stickiness at a macroscale level. Freeze-dried cakes and their corresponding powders were glassy and brittle, homogenous in color and free-flowing. Microcollapse phenomena occurring during freeze-concentration and detectable as budlike spherical domains, without any significant effect on the resulting powders at a macroscale level have been reported elsewhere (Heller et al., 1999; Johnson et al., 2010). Ice formation during freezing causes a concentration of solutes into a freeze-concentrated phase before the glass transition is reached, that in some cases can result in a thermodynamic propensity to phase separation.

3.8. Color

Microencapsulated powders had a light yellow to light brown color as shown by positive but low a^* and positive b^* values in the range +11 to 22 (Table 5). Higher concentration of OLE per mass unit, i.e. higher OLE:matrix, resulted in a more intense color as shown by higher values of the chromatic indices and lower L^* values. Colored compounds with apolar nature such as chlorophyll and derivatives or flavonols like luteolin are present in olive leaves (Flamminii et al., 2019; Rahmanian et al., 2015). OLE powders present, thus, a brown color that contributes, based on the relative concentration to the coloration of the microencapsulated powders and its intensity (Saikia et al., 2015).

Matrix component also appeared to play a role in the color of the powders. At equal OLE:matrix ratio, samples with maltodextrin as wall component and higher % solids showed a slightly more intense yellow

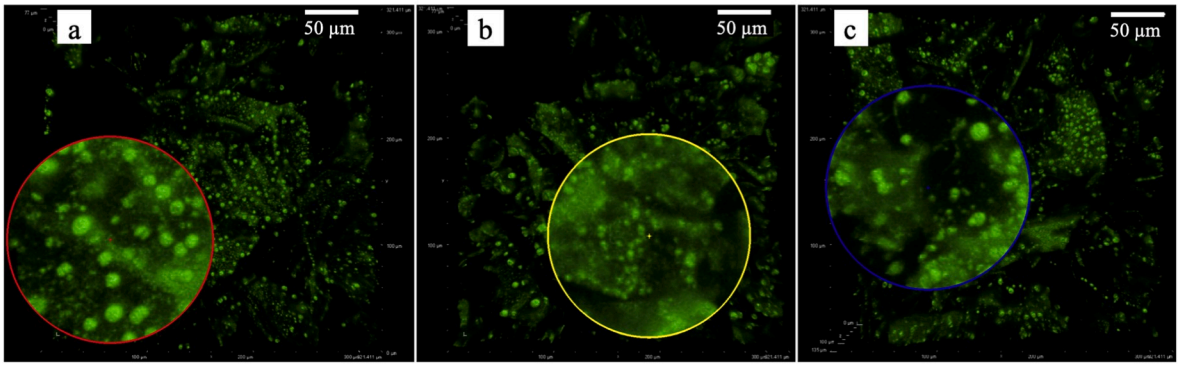

Fig. 3. CLSM micrographs of microencapsulated powders at OLE:matrix ratio = 0.25 and matrix composition (a) 100%MD, (b) 50%MD-50%TR and (c) 100%TR. Magnification: 40X, in 3D Z mode.

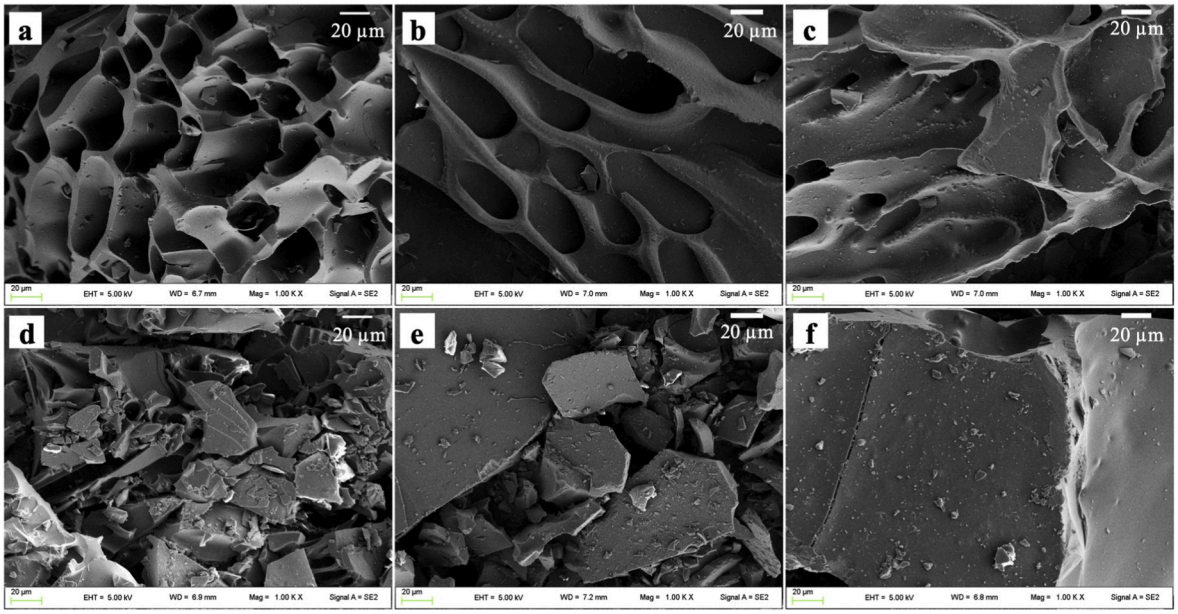

Fig. 4. SEM micrographs of control and microencapsulated OLE powders with 100%MD: (a) control, (b) OLE:matrix = 0.05 and (c) OLE:matrix = 0.25; and 100%TR: (d) control, (e) OLE:matrix = 0.05 and (f) OLE:matrix = 0.25.

Table 5
Colourimetric parameters and Yellow Index (YI) of microencapsulated powders.

EF	Experimental values of variables				Color			
	% solids (X_1)	MD:TR (X_2)		OLE:matrix (X_3)	L^*	a^*	b^*	YI
		%MD	%TR					
OLE	–	–	–	–	37.13 ±0.48^{a}	4.36 ±0.44^{g}	21.99 ±0.09^{g}	84.63 ±0.84^{i}
4	30	100	0	0.05	52.82 ±0.23^{f}	0.03 ±0.03^{a}	14.66 ±0.11^{c}	39.66 ±0.13^{c}
3	10	100	0	0.05	53.67 ±0.36^{fg}	0.06 ±0.01^{a}	13.45 ±0.30^{bc}	35.81 ±0.88^{bc}
2	30	0	100	0.05	54.18 ±0.24^{g}	0.10 ±0.01^{a}	13.02 ±0.29^{ab}	34.34 ±0.84^{ab}
1	10	0	100	0.05	55.32 ±0.38^{h}	0.13 ±0.02^{a}	11.90 ±0.13^{a}	30.74 ±0.54^{a}
8	30	100	0	0.25	46.07 ±0.55^{a}	2.41 ±0.12^{f}	21.73 ±0.33^{g}	67.41 ±1.67^{h}
7	10	100	0	0.25	47.64 ±0.46^{b}	1.88 ±0.04^{e}	19.31 ±0.58^{ef}	57.91 ±1.60^{fg}
6	30	0	100	0.25	47.00 ±0.37^{ab}	2.22 ±0.06^{f}	19.72 ±0.72^{f}	59.95 ±2.63^{g}
5	10	0	100	0.25	47.82 ±0.34^{bc}	1.84 ±0.16^{e}	18.72 ±0.36^{df}	55.94 ±0.75^{eg}
13	20	50	50	0.09	50.46 ±0.18^{e}	0.90 ±0.05^{b}	17.33 ±0.57^{d}	49.08 ±1.68^{d}
15	20	50	50	0.15	48.77 ±0.31^{cd}	1.49 ±0.09^{cd}	18.42 ±0.82^{df}	53.95 ±2.42^{def}
14	20	50	50	0.21	49.00 ±0.47^{d}	1.68 ±0.09^{de}	19.06 ±0.85^{ef}	55.60 ±3.01^{eg}
11	20	21	79	0.15	49.24 ±0.36^{d}	1.50 ±0.02^{cd}	18.21 ±0.36^{df}	52.83 ±1.00^{de}
12	20	79	21	0.15	49.20 ±0.26^{d}	1.45 ±0.04^{c}	18.17 ±0.60^{de}	52.76 ±1.86^{de}

Results are expressed as mean value of three replicate analysis ±SD.
Different superscript letters in the same column indicate significant differences at a probability level of $p < 0.05$.

color (i.e. higher b* and YI values and lower L*) than those with trehalose as wall components and lower % solids. This indicates a higher retention of OLE pigment compounds in maltodextrin-rich matrices. It has been demonstrated that saccharides with α-(1,4) glycoside link generates apolar surfaces, increasing their ability to bind apolar molecules (Sundari and Balasubramanian, 1997). Thus, since maltodextrin has α-(1,4) link and a higher molecular weight than trehalose, it is expected to interact and bind a higher fraction of such apolar pigments.

4. Conclusions

Results of this study showed the role of formulation variables e.g. matrix composition and complexity (single component vs. binary maltodextrin-trehalose mix) and core-to-matrix ratio, in affecting phenolics encapsulation of an olive leaf extract by freeze-drying. A design of experiments optimization approach using RSM was employed and results highlighted that the matrix composition and the amount of OLE had a significant effect on the encapsulation efficiency and the antioxidant, thermal, physical and microstructural properties of the freeze-dried encapsulated powders. The increasing concentration of maltodextrin enhanced the encapsulation of both OLE total phenolics and oleuropein up to an almost total retention when MD is used alone, which could be directly observed thanks to fluorescence imaging. Color and thermal properties of the microencapsulated powders depend on the maltodextrin-trehalose ratio and a plasticizing effect of OLE was also observed, especially in the glassy powders containing MD. Surface structure observations obtained by electron microscopy showed significant differences in shape and morphology among samples with different matrix composition and the effect of the OLE presence.

Results of this study allow the evaluation of formulation variables on freeze-drying encapsulation and powder properties using matrix binary systems of high and low molecular weight carbohydrates (i.e. maltodextrin and trehalose) good glass formers and representatives of many food systems in which they could be incorporated. In particular, the feasibility of freeze-drying to obtain microencapsulates characterized by a high retention of the OLE bioactives when MD is the prevalent matrix

component was evidenced. The role of trehalose used either as single carrier component or mixed with MD need to be better understood with main reference to the physical and chemical stability during storage and under different environmental conditions. Further studies are also required to evaluate the technological applications of the OLE extracts in complex food formulation and their impact on quality, sensory (e.g. bitterness) and stability.

Declaration of competing interest

None.

CRediT authorship contribution statement

Rodrigo González-Ortega: Investigation, Formal analysis, Writing - original draft. **Marco Faieta:** Supervision, Visualization. **Carla D. Di Mattia:** Methodology, Writing - review & editing. **Luca Valbonetti:** Investigation, Resources. **Paola Pittia:** Conceptualization, Writing - review & editing, Funding acquisition, Project administration.

Acknowledgments

This work was supported by Italian Ministry of University and Research and has received funding from the European Union's Horizon 2020 research and innovation program under the Marie Skłodowska-Curie grant agreement *N*° 713714. The authors would like to thank Alessandro di Michele for performing the SEM analysis, and also OLEAFIT S.r.l (Isola del Gran Sasso, Italy) for kindly providing the olive leaf powder extract.

References

Ahmad-Qasem, Margarita, H., Ahmad-Qasem, B.H., Barrajón-Catalán, E., Micol, V., Cárcel, J.A., García-Pérez, J.V., 2016. Drying and storage of olive leaf extracts. Influence on polyphenols stability. Ind. Crop. Prod. 79, 232–239. https://doi.org/10.1016/j.indcrop.2015.11.006.

Ahmad-Qasem, Hussam, Margarita, Barrajón-Catalán, E., Micol, V., Mulet, A., García-Pérez, J.V., 2013. Influence of freezing and dehydration of olive leaves (var. Serrana) on extract composition and antioxidant potential. Food Res. Int. 50 (1), 189–196. https://doi.org/10.1016/j.foodres.2012.10.028.

Aliakbarian, B., Sampaio, F.C., de Faria, J.T., Pitangui, C.G., Lovaglio, F., Casazza, A.A., et al., 2018. Optimization of spray drying microencapsulation of olive pomace polyphenols using Response Surface Methodology and Artificial Neural Network. LWT 93, 220–228. https://doi.org/10.1016/j.lwt.2018.03.048.

Amoako, D., Awika, J.M., 2016. Polyphenol interaction with food carbohydrates and consequences on availability of dietary glucose. Curr. Opin. Food Sci. 8, 14–18.

Aouidi, F., Okba, A., Hamdi, M., 2017. Valorization of functional properties of extract and powder of olive leaves in raw and cooked minced beef meat. J. Sci. Food Agric. 97 (10), 3195–3203. https://doi.org/10.1002/jsfa.8164.

Avaltroni, F., Bouquerand, P.E., Normand, V., 2004. Maltodextrin molecular weight distribution influence on the glass transition temperature and viscosity in aqueous solutions. Carbohydr. Polym. 58 (3), 323–334.

Ballesteros, L.F., Ramirez, M.J., Orrego, C.E., Teixeira, J.A., Mussatto, S.I., 2017. Encapsulation of antioxidant phenolic compounds extracted from spent coffee grounds by freeze-drying and spray-drying using different coating materials. Food Chem. 237, 623–631.

Chanioti, S., Siamandoura, P., Tzia, C., 2016. Evaluation of extracts prepared from olive oil by-products using microwave-assisted enzymatic extraction: effect of encapsulation on the stability of final products. Waste Biomass Valoriz. 7 (4), 831–842. https://doi.org/10.1007/s12649-016-9533-1.

Che Man, Y.B., Irwandi, J., Abdullah, W.J.W., 1999. Effect of different types of maltodextrin and drying methods on physico-chemical and sensory properties of encapsulated durian flavour. J. Sci. Food Agric. 79 (8), 1075–1080.

Chen, H., Tian, M., Chen, L., Cui, X., Meng, J., Shu, G., 2019. Optimization of composite cryoprotectant for freeze-drying Bifidobacterium bifidum BB01 by response surface methodology. Artificial Cells, Nanomed. Biotechnol. 47 (1), 1559–1569.

Desobry, S.A., Netto, F.M., Labuza, T.P., 1997. Comparison of spray-drying, drum-drying and freeze-drying for β-carotene encapsulation and preservation. J. Food Sci. 62 (6), 1158–1162.

Di Francesco, A., Falconi, A., Di Germanio, C., Di Bonaventura, M.V.M., Costa, A., Caramuta, S., et al., 2015. Extravirgin olive oil up-regulates CB1 tumor suppressor gene in human colon cancer cells and in rat colon via epigenetic mechanisms. J. Nutr. Biochem. 26 (3), 250–258.

Difonzo, G., Russo, A., Trani, A., Paradiso, V.M., Ranieri, M., Pasqualone, A., et al., 2017. Green extracts from Coratina olive cultivar leaves: antioxidant characterization and biological activity. J. Funct. Foods 31 (January), 63–70. https://doi.org/10.1016/j.jff.2017.01.039.

Faieta, M., Corradini, M.G., Di Michele, A., Ludescher, R.D., Pittia, P., 2019. Effect of encapsulation process on technological functionality and stability of spirulina platensis extract. Food Biophys. 1–14.

Flamminii, F., Di Mattia, C.D., Difonzo, G., Neri, L., Faieta, M., Caponio, F., Pittia, P., 2019. From by-product to food ingredient: evaluation of compositional and technological properties of olive-leaf phenolic extracts. J. Sci. Food Agric. https://doi.org/10.1002/jsfa.9949.

Francis, F.J., Clydesdale, F.M., 1975. Food Colorimetry: Theory and Applications. AVI Publishing Co. Inc.

Ganje, M., Jafari, S.M., Dusti, A., Dehnad, D., Amanjani, M., Ghanbari, V., 2016. Modeling quality changes in tomato paste containing microencapsulated olive leaf extract by accelerated shelf life testing. Food Bioprod. Process. 97, 12–19. https://doi.org/10.1016/j.fbp.2015.10.002.

Gharsallaoui, A., Roudaut, G., Chambin, O., Voilley, A., Saurel, R., 2007. Applications of spray-drying in microencapsulation of food ingredients: an overview. Food Res. Int. 40 (9), 1107–1121.

González, E., Gómez-Caravaca, A.M., Giménez, B., Cebrián, R., Maqueda, M., Martínez-Férez, A., et al., 2019. Evolution of the phenolic compounds profile of olive leaf extract encapsulated by spray-drying during in vitro gastrointestinal digestion. Food Chem. 279, 40–48. https://doi.org/10.1016/j.foodchem.2018.11.127.

Harnkarnsujarit, N., Charoenrein, S., Roos, Y.H., 2012. Microstructure formation of maltodextrin and sugar matrices in freeze-dried systems. Carbohydr. Polym. 88 (2), 734–742.

Heller, M.C., Carpenter, J.F., Randolph, T.W., 1999. Application of a thermodynamic model to the prediction of phase separations in freeze-concentrated formulations for protein lyophilization. Arch. Biochem. Biophys. 363 (2), 191–201.

Igual, M., Ramires, S., Mosquera, L.H., Martínez-Navarrete, N., 2014. Optimization of spray drying conditions for lulo (Solanum quitoense L.) pulp. Powder Technol. 256, 233–238.

Johnson, R.E., Oldroyd, M.E., Ahmed, S.S., Gieseler, H., Lewis, L.M., 2010. Use of manometric temperature measurements (MTM) to characterize the freeze-drying behavior of amorphous protein formulations. J. Pharmaceut. Sci. 99 (6), 2863–2873.

Kalichevsky, M.T., Blanshard, J.M.V., 1992. A study of the effect of water on the glass transition of 1: 1 mixtures of amylopectin, casein and gluten using DSC and DMTA. Carbohydr. Polym. 19 (4), 271–278.

Kilburn, D., Claude, J., Schweizer, T., Alam, A., Ubbink, J., 2005. Carbohydrate polymers in amorphous states: an integrated thermodynamic and nanostructural investigation. Biomacromolecules 6 (2), 864–879.

Kosaraju, S.L., D'ath, L., Lawrence, A., 2006. Preparation and characterisation of chitosan microspheres for antioxidant delivery. Carbohydr. Polym. 64 (2), 163–167. https://doi.org/10.1016/j.carbpol.2005.11.027.

Laine, P., Kylli, P., Heinonen, M., Jouppila, K., 2008. Storage stability of microencapsulated cloudberry (Rubus chamaemorus) phenolics. J. Agric. Food Chem. 56 (23), 11251–11261.

Laokuldilok, T., Kanha, N., 2017. Microencapsulation of black glutinous rice anthocyanins using maltodextrins produced from broken rice fraction as wall material by spray drying and freeze drying. J. Food Process. Preserv. 41 (1), 1–10. https://doi.org/10.1111/jfpp.12877.

Leopoldini, M., Russo, N., Toscano, M., 2011. The molecular basis of working mechanism of natural polyphenolic antioxidants. Food Chem. 125 (2), 288–306. https://doi.org/10.1016/j.foodchem.2010.08.012.

Maidannyk, V.A., Nurhadi, B., Roos, Y.H., 2017. Structural strength analysis of amorphous trehalose-maltodextrin systems. Food Res. Int. 96, 121–131. https://doi.org/10.1016/j.foodres.2017.03.029.

Martín-Peláez, S., Covas, M.I., Fitó, M., Kušar, A., Pravst, I., 2013. Health effects of olive oil polyphenols: recent advances and possibilities for the use of health claims. Mol. Nutr. Food Res. 57 (5), 760–771. https://doi.org/10.1002/mnfr.201200421.

Michalska, A., Lech, K., 2018. The effect of carrier quantity and drying method on the physical properties of apple juice powders. Beverages 4 (1), 2.

Mohammadi, A., Jafari, S.M., Esfanjani, A.F., Akhavan, S., 2016. Application of nano-encapsulated olive leaf extract in controlling the oxidative stability of soybean oil. Food Chem. 190, 513–519. https://doi.org/10.1016/j.foodchem.2015.05.115.

Mouratoglou, E., Malliou, V., Makris, D.P., 2016. Novel glycerol-based natural eutectic mixtures and their efficiency in the ultrasound-assisted extraction of antioxidant polyphenols from agri-food waste biomass. Waste Biomass Valoriz. 7 (6), 1377–1387. https://doi.org/10.1007/s12649-016-9539-8.

Mourtzinos, I., Salta, F., Yannakopoulou, K., Chiou, A., Karathanos, V.T., 2007. Encapsulation of olive leaf extract in β-cyclodextrin. J. Agric. Food Chem. 55 (20), 8088–8094. https://doi.org/10.1021/jf0709698.

Munin, A., Edwards-Lévy, F., 2011. Encapsulation of natural polyphenolic compounds; a review. Pharmaceutics 3 (4), 793–829.

Myers, R.H., Montgomery, D.C., Anderson-Cook, C.M., 2016. Response Surface Methodology: Process and Product Optimization Using Designed Experiments. John Wiley & Sons.

Nurhadi, B., Roos, Y.H., Maidannyk, V., 2016. Physical properties of maltodextrin DE 10: water sorption, water plasticization and enthalpy relaxation. J. Food Eng. 174, 68–74.

Paini, M., Aliakbarian, B., Casazza, A.A., Lagazzo, A., Botter, R., Perego, P., 2015. Microencapsulation of phenolic compounds from olive pomace using spray drying: a study of operative parameters. LWT - Food Sci. Technol. (Lebensmittel-Wissenschaft -Technol.) 62 (1), 177–186. https://doi.org/10.1016/j.lwt.2015.01.022.

Paradiso, V.M., Clemente, A., Summo, C., Pasqualone, A., Caponio, F., 2016. Towards green analysis of virgin olive oil phenolic compounds: extraction by a natural deep eutectic solvent and direct spectrophotometric detection. Food Chem. 212, 43–47.

Pasrija, D., Ezhilarasi, P.N., Indrani, D., Anandharamakrishnan, C., 2015. Microencapsulation of green tea polyphenols and its effect on incorporated bread quality. LWT - Food Sci. Technol. (Lebensmittel-Wissenschaft -Technol.) 64 (1), 289–296. https://doi.org/10.1016/j.lwt.2015.05.054.

Patist, A., Zoerb, H., 2005. Preservation mechanisms of trehalose in food and biosystems. Colloids Surf. B Biointerfaces 40 (2), 107–113.

Paulo, F., Santos, L., 2017. Design of experiments for microencapsulation applications: a review. Mater. Sci. Eng. C 77, 1327–1340.

Potes, N., Kerry, J.P., Roos, Y.H., 2012. Additivity of water sorption , alpha-relaxations and crystallization inhibition in lactose – maltodextrin systems. Carbohydr. Polym. 89 (4), 1050–1059. https://doi.org/10.1016/j.carbpol.2012.03.061.

Pravinata, L.C., Murray, B.S., 2019. Encapsulation of water-insoluble polyphenols and β-carotene in Ca-alginate microgel particles produced by the Leeds Jet Homogenizer. Colloid. Surface. Physicochem. Eng. Aspect. 561, 147–154. https://doi.org/10.1016/j.colsurfa.2018.10.041.

Rahmanian, N., Jafari, S.M., Wani, T.A., 2015. Bioactive profile, dehydration, extraction and application of the bioactive components of olive leaves. Trends Food Sci. Technol. 42 (2), 150–172. https://doi.org/10.1016/j.tifs.2014.12.009.

Ramírez, M.J., Giraldo, G.I., Orrego, C.E., 2015. Modeling and stability of polyphenol in spray-dried and freeze-dried fruit encapsulates. Powder Technol. 277, 89–96.

Ravichai, K., Muangrat, R., 2019. Effect of different coating materials on freeze-drying encapsulation of bioactive compounds from fermented tea leaf wastewater. J. Food Process. Preserv. 43 (10), e14145. https://doi.org/10.1111/jfpp.14145.

Re, R., Pellegrini, N., Proteggente, A., Pannala, A., Yang, M., Rice-Evans, C., 1999. Antioxidant activity applying an improved ABTS radical cation decolorization assay. Free Radic. Biol. Med. 26 (9–10), 1231–1237.

Robert, P., Gorena, T., Romero, N., Sepulveda, E., Chavez, J., Saenz, C., 2010. Encapsulation of polyphenols and anthocyanins from pomegranate (Punica granatum) by spray drying. Int. J. Food Sci. Technol. 45 (7), 1386–1394.

Roos, Y.H., 2010. 25 crystallization, collapse, and glass transition in low-water food systems. In: Water Properties in Food, Health, Pharmaceutical and Biological Systems: ISOPOW, vol. 10, p. 335.

Roos, Yrjo H., Drusch, S., 2015. Phase Transitions in Foods. Academic Press.

Roos, Yrjö H., Livney, Y.D., 2017. Engineering Foods for Bioactives Stability and Delivery. Springer.

Roos, Yrjo, Karel, M., 1990. Differential scanning calorimetry study of phase transitions affecting the quality of dehydrated materials. Biotechnol. Prog. 6 (2), 159–163.

Roos, Yrjö, Karel, M., 1991a. Phase transitions of mixtures of amorphous polysaccharides and sugars. Biotechnol. Prog. 7 (1), 49–53.

Roos, Yrjö, Karel, M., 1991b. Water and molecular weight effects on glass transitions in amorphous carbohydrates and carbohydrate solutions. J. Food Sci. 56 (6), 1676–1681.

Ruiz-Moreno, M.J., Raposo, R., Moreno-Rojas, J.M., Zafrilla, P., Cayuela, J.M., Mulero, J., et al., 2015. Efficacy of olive oil mill extract in replacing sulfur dioxide in wine model. LWT Food Sci. Technol. 61 (1), 117–123.

Saavedra-Leos, M.Z., Leyva-Porras, C., Martínez-Guerra, E., Pérez-García, S.A., Aguilar-Martínez, J.A., Álvarez-Salas, C., 2014. Physical properties of inulin and inulin-orange juice: physical characterization and technological application. Carbohydr. Polym. 105 (1), 10–19. https://doi.org/10.1016/j.carbpol.2013.12.079.

Sacchetti, G., Di Mattia, C., Pittia, P., Mastrocola, D., 2009. Effect of roasting degree, equivalent thermal effect and coffee type on the radical scavenging activity of coffee brews and their phenolic fraction. J. Food Eng. 90 (1), 74–80.

Saikia, S., Mahnot, N.K., Mahanta, C.L., 2015. Optimisation of phenolic extraction from Averrhoa carambola pomace by response surface methodology and its microencapsulation by spray and freeze drying. Food Chem. 171, 144–152.

Sajadi, M., Ajaj, Y., Ioffe, I., Weingärtner, H., Ernsting, N.P., 2010. Terahertz absorption spectroscopy of a liquid using a polarity probe: a case study of trehalose/water mixtures. Angew. Chem. Int. Ed. 49 (2), 454–457.

Sikorska, E., Khmelinskii, I., Sikorski, M., 2012. Analysis of olive oils by fluorescence spectroscopy: methods and applications. Olive Oil Const. Qual. Health Prop. Bioconvers. 63–87.

Sosa, N., Zamora, M.C., Chirife, J., Schebor, C., 2011. Spray-drying encapsulation of citral in sucrose or trehalose matrices: physicochemical and sensory characteristics. Int. J. Food Sci. Technol. 46 (10), 2096–2102.

Souilem, S., Fki, I., Kobayashi, I., Khalid, N., Neves, M.A., Isoda, H., et al., 2017. Emerging technologies for recovery of value-added components from olive leaves and their applications in food/feed industries. Food Bioprocess Technol. 10 (2), 229–248.

Sundari, C.S., Balasubramanian, D., 1997. Hydrophobic surfaces in saccharide chains. Prog. Biophys. Mol. Biol. 67 (2–3), 183–216.

Talhaoui, N., Taamalli, A., Gómez-Caravaca, A.M., Fernández-Gutiérrez, A., Segura-Carretero, A., 2015. Phenolic compounds in olive leaves: analytical determination, biotic and abiotic influence, and health benefits. Food Res. Int. 77, 92–108. https://doi.org/10.1016/j.foodres.2015.09.011.

Te, J.A., Tan, M.-L., Ichiye, T., 2010. Solvation of glucose, trehalose, and sucrose by the soft-sticky dipole–quadrupole–octupole water model. Chem. Phys. Lett. 491 (4–6), 218–223.

Urzúa, C., González, E., Dueik, V., Bouchon, P., Giménez, B., Robert, P., 2017. Olive leaves extract encapsulated by spray-drying in vacuum fried starch–gluten doughs. Food Bioprod. Process. 106, 171–180.

Xynos, N., Papaefstathiou, G., Gikas, E., Argyropoulou, A., Aligiannis, N., Skaltsounis, A.-L., 2014. Design optimization study of the extraction of olive leaves performed with pressurized liquid extraction using response surface methodology. Separ. Purif. Technol. 122, 323–330. https://doi.org/10.1016/j.seppur.2013.10.040.

Zhou, Y., Roos, Y.H., 2012. Stability and plasticizing and crystallization effects of vitamins in amorphous sugar systems. J. Agric. Food Chem. 60 (4), 1075–1083. https://doi.org/10.1021/jf204168f.